REPORT DOCUMENTATION PAGE

Form Approved
OMB No. 0704-0188

1. AGENCY USE ONLY (Leave blank)

2. REPORT DATE: 10, May 1997

3. REPORT TYPE AND DATES COVERED: Final Report 15 Aug. 1996 to 14 Feb. 1997

4. TITLE AND SUBTITLE: High Rate Sputter Deposition Method for Superconductors

5. FUNDING NUMBERS: 62173C 1660/01

6. AUTHOR(S): Curtis M. Lampkin

7. PERFORMING ORGANIZATION NAME(S) AND ADDRESS(ES):
Solar Associates
710 Venetian Way
Merritt Island, FL 32953

AFOSR-TR-97

0182

9. SPONSORING/MONITORING AGENCY NAME(S) AND ADDRESS(ES):
AFOSR/NE
Directorate of Physics & Electronics
110 Duncan Ave. Bolling AFB, DC 20332-8080

10. SPONSORING/MONITORING AGENCY REPORT NUMBER: F49620-96-C-0045

11. SUPPLEMENTARY NOTES

19970602 134

12a. DISTRIBUTION/AVAILABILITY STATEMENT

APPROVED FOR PUBLIC RELEASE: DISTRIBUTION UNLIMITED

13. ABSTRACT (Maximum 200 words) Magnetron sputtering deposition is potentially the most economical deposition method for thin films. Presently sputtering can't deposit high temperature superconductors like Yttrium Barium Copper Oxide (YBCO) because of negative oxygen ion bombardment damage. Lowering the plasma discharge voltage to less than 100 volts would decrease such damage and make YBCO economically practical. The goal of this phase I effort was to lower plasma discharge voltages using high magnetic fields. Our results showed that high magnetic fields alone can lower plasma voltages to about 200 volts. Just as important, we showed that plasma impedance was lowered by more than ten times. Low plasma impedance allows high magnetic fields and electron injection into the plasma to be combined to lower plasma voltage to 30 volts. This combination removes the power limitations of electron injection. It should also produce epitaxial quality thin film semiconductors because low voltages allow "self-bombardment" where the adatoms have the optimum energy to form a crystalline matrix at lower temperatures. The method is also applicable to thin film semiconductors such as II-VI solar cells and III-V films.

14. SUBJECT TERMS: Negative Ion Bombardment, Magnetron Sputtering, YBCO, High Temperature Superconductors, Low Plasma Discharge Voltage

15. NUMBER OF PAGES: 30

16. PRICE CODE

17. SECURITY CLASSIFICATION OF REPORT	18. SECURITY CLASSIFICATION OF THIS PAGE	19. SECURITY CLASSIFICATION OF ABSTRACT	20. LIMITATION OF ABSTRACT
Unclassified	Unclassified	Unclassified	None

NSN 7540-01-280-5500

DTIC QUALITY INSPECTED 1

Standard Form 298 (Rev. 2-89)
Prescribed by ANSI Std. Z39-18
298-102

Final Phase I Report for SBIR Contract # F49620-96-C-0045

Sponsored by BMDO
Organization: Solar Associates
Principal Investigator: Curt M. Lampkin
Report date: May 10, 1997

Contract Title: "High Rate Sputter Deposition Method for Superconductors"

Table of Contents

Introduction

Magnetron sputtering is the most economical method for extremely large scale physical vapor deposition of thin films. Other methods, such as e-beam evaporation, cannot, under present circumstances, economically make the high film quality needed for such markets as architectural thin films. CVD is the main competition to sputtering for architectural films but its range of materials is more limited and it has serious environmental concerns. The low costs, high film quality and rapid deposition rates of magnetron sputtering have attracted many other markets to attempt its use .

The defining aspect of a magnetron is the magnetic field behind the target surface. This field captures and traps electrons by forcing them into helical and cycloidal paths. These helical paths are much longer than the straight line paths which untrapped electrons would travel. This lengthed path increases the collision frequency of electrons with argon atoms. More argon atoms are positively ionized at lower plasma voltages. High deposition rates and favorable energy are among the main attractions of magnetron sputtering.

Some markets attempting to use sputtering are high temperature superconductors such as thin film Yttrium Barium Copper Oxide (YBCO) and thin film solar cells made from chalcogenides such as Copper Indium Diselenide (CIS) and Cadmium Telluride (CdTe). These materials could possibly be made more economically and rapidly by sputtering than by any other method. Chalcogenides are compounds containing a chalcogen: Oxygen, Sulfur, Selenium , or Tellurium. Presently, no one is able to economically sputter YBCO or other chalcogenides .

Magnetron sputtering is well suited for deposition of metals and metal oxides and it dominates those markets. Oxygen is well behaved with many metals. However, when some materials are sputtered along with a chalcogen a serious problem can arise. Such materials can easily lose electrons to form negative chalcogen ions which are repelled from the negatively charged sputtering target. In the case of YBCO, the barium metal in it has a low electron affinity and easily gives up an electron to any nearby oxygen molecules to form negative oxygen ions. Since the sputtering target is negatively biased, the negative oxygen ions are repelled with an energy equal to the target plasma discharge voltage

As the oxygen ions travel to the substrate, they are neutralized in the plasma zone but they still retain all of their energy. They travel directly to the substrate and damage the thin films being deposited there. Negative oxygen ions can bombard sputtered YBCO with such force that they etch away the YBCO film ,and in many cases, part of the substrate itself. In the case of chalcogenide thin film solar cells, the Tellurium and Selenium atoms become negatively ionized and damage the solar cell.

Negative Ion bombardment, also called reflected high energy neutral bombardment, has been studied by several investigators. Geerk, et al [1] have used off axis sputtering as well as inverted magnetron sputtering where the material normally wasted is partially recollected on an opposing magnetron. Gavaler et. al. [2] have shown that while ion bombardment must be eliminated there are other parameters which also affect film quality such as the activation state of the oxygen used. Cuomo [3] shows that negative ion bombardment will probably exist with all chalcogens. Hammond [4], in an initial estimate for high rate production of YBCO on tape, does not even consider sputtering but instead proposes e-beam co-evaporation. There are many large and promising markets for sputtering if negative ion bombardment can be eliminated.

Presently there are two remedies for oxygen ion bombardment used in YBCO sputtering. Both have economic penalties. First, the substrate can be placed to one side of the target and coated indirectly. This avoids the negative ions which travel directly from the target. However it slows the deposition rate and wastes most of the material. Second, a high sputtering pressure can be used. This causes an ion to collide with several gas molecules before it reaches the substrate. The multiple collisions remove most of the ion energy and the damage is avoided. This high pressure also wastes material by gas scattering and can hinder oxygen pressure control needed to maintain stoichiometry.

There is another remedy for negative ion bombardment which has not been widely used until now because of technical obstacles. That remedy is to use a plasma discharge voltage of 50 volts or less.

Since the voltage is so low no negative ion can gain enough energy to damage the film. There are 2 ways to achieve lower plasma discharge voltage.

First, electrons can be injected directly into the sputter plasma zone using hollow cathode or thermionic emitters. Such devices are offered on the market. [5]. Howson [6] achieved a 100 volt plasma with a tungsten filament, while Cuomo and Rossnagle [7] showed that plasma voltages of 30 volts could be achieved with a hollow cathode emitter. But electron injection has had disadvantages that precluded its general use.

Most of the injected electrons are poorly contained and quickly lost. The result of electron loss is that magnetron current is severely limited, to about 20 % of the injected current. Above the 20% limit the plasma voltage increases markedly[7]. Unless care is taken to provide a suitable anode for the electron gun, the plasma can be non-uniform with plasma intensity and deposition rate decreasing away from the electron injection point.

The second method is the use of high magnetic fields to contain the plasma. Thornton [8] and Wendt and Lieberman [9] show that voltage decreases as magnetic field strength increases. Ishibashi et al [10] reported that plasma voltages of 80 volts were achieved at an unspecified magnetic field strength. The disadvantage here is that voltages, Ishibashi excepted, were limited to several hundred volts. I have not yet been able to find duplication of Ishibashi's work in the literature and the experimental details given in his paper were insufficient for me to repeat the experiment.

High magnetic fields are usually a disadvantage with planar magnetrons since they form narrow grooves in the magnetron target surface and drastically reduced material usage efficiency. Targets must then be changed much more often. Usually, planar magnetrons have weaker magnetic fields, of from 200 to 400 gauss. Weak fields keep the plasma etch groove wide and shallow. This provide higher material usage and the targets last longer. Material usage is about 25 to 30% for planar magnetrons

I have recently invented (patent # 5,405,517) a new type of magnetron, called the surrogate magnetron. It allows the use of very high magnetic fields for sputtering.

The surrogate magnetron evolved from the rotating cylindrical magnetron. which in turn evolved from the planar magnetron. Figure 1 shows a standard planar magnetron

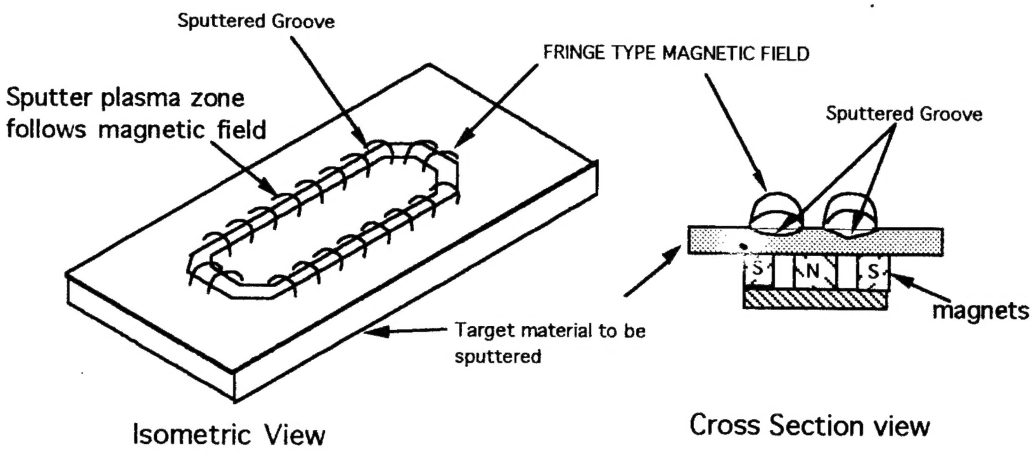

Figure 1 A planar magnetron

Because the gap between poles collects most of the flux it is difficult to obtain high strength magnetic fields which "fringe" above the target surface. The further you get from the magnets themselves the weaker the magnetic flux becomes. Standard magnetron targets are precoated with any where from 6 to 20 millimeters of material depending on magnetron size and power rating. The "coatings" are usually solid castings or pressed billets of material which are bonded to a water cooled copper backing plate This material separates the magnet from the target surface. Higher strength fringing magnetic fields are possible with thinner magnetron targets where the magnet is closer to the target surface. But thin targets are uneconomical since they must be changed often.

Target utilization has been improved with the rotating cylindrical magnetron shown in the next figure .

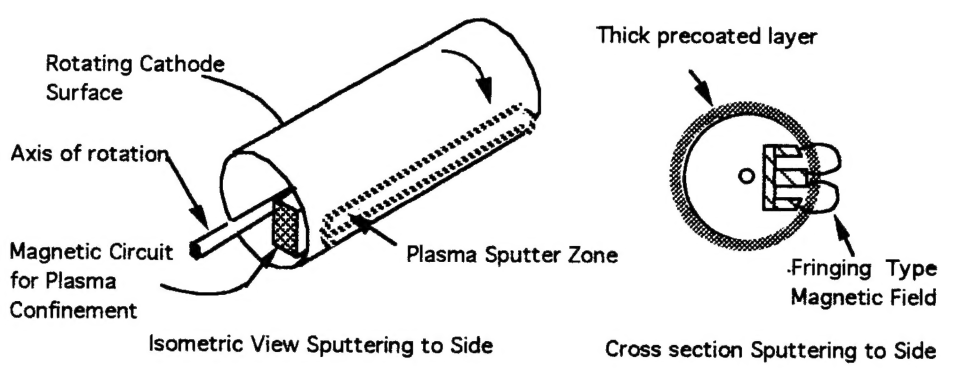

Figure 2.. A rotating cylindrical magnetron

Here a rotating cylindrical target continually moves material through the plasma zone. The material to be sputtered is sometimes precoated onto the cylindrical surface by plasma spraying.

Or the target surface can be made from a single piece of self-supporting metal such as copper, aluminum or titanium.

The precoated material can be thinner here but it is still in the range of 3 to 12 millimeters. Material usage is as high as 80% and the narrow grooves caused by high fields do not form. As with the planar magnetron, the target thickness of this rotating magnetron decreases as the material is eroded. Thus the magnetic field continually increases during target use. This makes process control more difficult. As will be shown later, field strength is a logarithmic function of magnet to surface distance thickness. To get the strongest fields, the target wall thickness must be on the order of one or two millimeters including the material to be sputtered, the target backing structure and running clearances.

Targets for cylindrical magnetrons are difficult to make. Available materials are limited, and often expensive. The precoated material should be a good thermal conductor such as a metal. If a compound or semiconductor are used then the power to the target is limited and the process is more expensive since more targets are needed.

The surrogate magnetron type is shown next in figure 3. The surrogate magnetron is similar to the rotating cylindrical magnetron with one important difference. The surrogate is not precoated at all. Instead, it is coated in the vacuum chamber during the deposition process. One or more auxiliary sources are placed around the surrogate magnetron to coat it with the necessary materials. These sources can be e-guns, vapor ovens, other magnetrons, or CVD deposition chambers. Since the surrogate is coated in the deposition system, stoichiometry, i.e. the ratio of the separate elements, can be controlled with high precision. No expensive targets are needed.

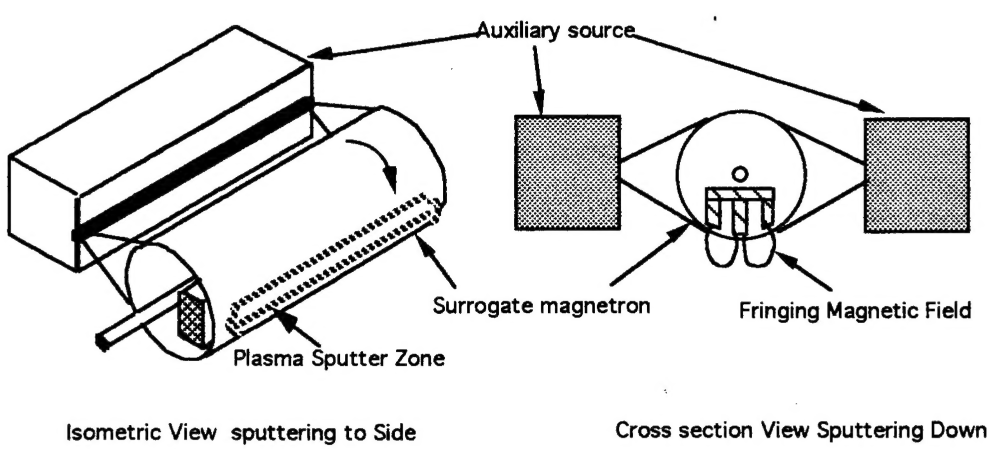

Figure 3 A surrogate magnetron

While additional sources might seem to complicate the configuration, the advantages more than compensate. The auxiliary sources and the surrogate together have such a high deposition rate that they can substitute for an even greater number of standard magnetrons.

Because the surrogate is coated continuously in-place, the coatings on it are thin, on the order of 10 to 100 microns. Such thin coatings don't add much to the 1.5 mm thick cylinder wall itself. Including 0.4 mm clearance to the magnet results in a total gap of about 2 mm. Such thin coatings have two advantages. First, thermal conductivity is very high. This allows one target to deposit as much material as several conventional targets. Second, thin coating allow the use of high magnetic fields.

The following figure 4 has a plot of B vs. distance. We see that a 2 mm gap allows a field of 5500 gauss. This plot of magnetic field vs. distance from the magnetic a vital design aid and allows estimation of the true surface magnetic fields. Figure 4 is a simulated field gradient generated by computer using software described later. It represents the design limits for NdFeB 40 H and this particular design configuration. Improved materials and designs could certainly increase the achievable field. It is easy to see that without the surrogate magnetron concept, such high magnetic fields are neither practical nor useful.

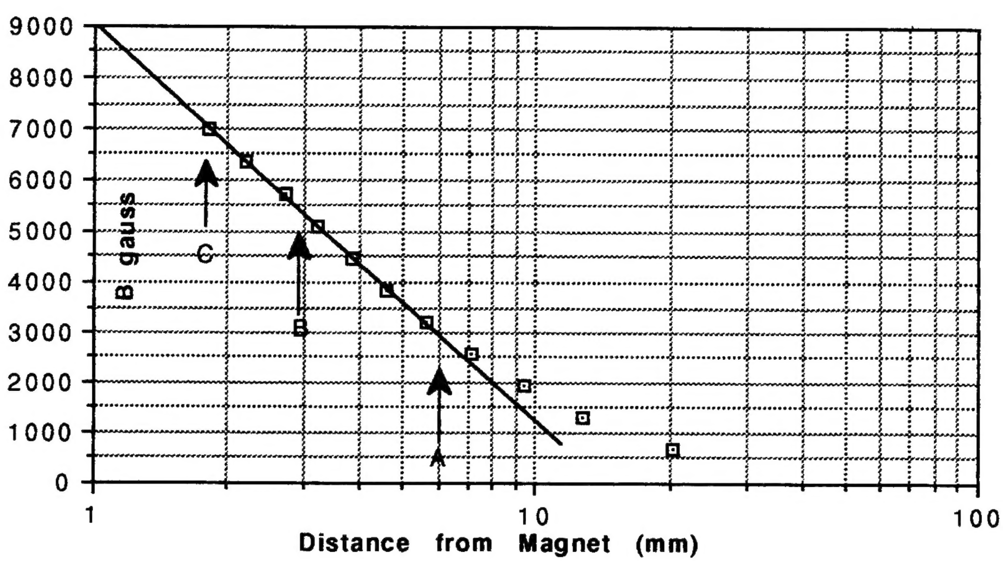

Figure 4 Design plot of B field vs distance

The major goals of this SBIR phase I contract were to:

1. Design and build a magnetron having a field of 10,000 gauss
2. With this high field demonstrate a plasma voltage of 100 volts or less
3. Design and build probes to measure the average energy of the atoms arriving at the substrate and the amount of high energy neutral atoms.
4. Deposit chromium at 100 volts or less to show the effects of low plasma V on chromium resistivity.

These are the results of this contract effort:

1. Magnets were designed with fields up to 7500 gauss.
2. An operating magnetron was built having a field of 5500 gauss.
3. Plasma voltage was lowered from the 500 to 600 volts range to 200 to 250 volts depending on the material.
4. The resulting plasma I-V plots showed that plasma impedance was reduced more than 10 times less than standard magnetrons with or without electron injection. The I-V curves are shown in the results section.
5. The energy probe was built and showed that there was moderate electron and ion bombardment of the substrate with these higher fields. This is the "unbalanced magnetron" effect. This might be further reduced with more effort to balance the fields.

The commercial implications of these results are impressive. The most important result is the achievement of low plasma impedance. Impedance is the ratio of voltage change to current change. Low impedance means that even though the magnetron current varies greatly, the plasma voltage remains nearly constant. Electron containment is much more efficient with these high magnetic fields. Some promising commercial possibilities are listed here

1. Low impedance and efficient electron containment make electron injection into the plasma practical. The current limitation and non-uniform plasma effects are eliminated. Plasma voltages down to 30 volts are now possible with the combination of electron injection and high magnetic fields.
2. Such low plasma voltages allow "self bombardment" to occur. Mueller [11] predicts that as these low energy levels are achieved, the arriving atoms will have the optimum energy to form epitaxial layers at low deposition temperatures. 1 electron volt is equivalent to 11,600 degrees K.

   There are several ways to add part of this beneficial energy. One is heating the substrate during deposition. Window and Savides [12] invented another method by using argon ion bombardment generated by unbalanced magnetrons. Ion beam assisted deposition (IBAD) also is a start in this direction of giving the proper energy to the atoms arriving at the substrate.

It seems reasonable to infer that adding energy with third body particles such as argon atoms is inferior to giving the arriving atoms themselves the correct energy to start with. And this correct energy can be supplied with a low voltage plasma

3. Lower deposition temperatures for YBCO films would allow lower cost lower temperature substrates to be used .
4. On-axis sputtering could be used for YBCO deposition. Rates will be much higher and this could provide the necessary impetus to bring YBCO films into many more of the market place opportunities than now exist.
5. Electron injection and high fields would allow the sputtering process to be carried out at much lower pressures. Lower pressures will tend to increase plasma voltages and it is a trade-off. But there are situations which can profit from low pressure. Lift-off mask lithography is one such area.
6. The surrogate magnetron allows elements to be used directly. Tellurium , Selenium and even Sulfur, with proper target cooling, can be used directly in elemental form instead of in the form of a poisonous gas. Hydrogen telluride, hydrogen selenide and hydrogen sulfide are extremely toxic and expensive to use. This is an important environmental cost consideration.

While solar cell development may seem somewhat unrelated to high temperature superconductor development, solar cells are a larger potential market at present. And there is a related benefit. The YBCO process development can aid the development of chalcogenide thin film solar cells such as CdTe and CIS which suffer the same ion bombardment problem. CdTe and CIS are very efficient, long-lived, proven, solar cell materials which have not yet reached the market place because of lack of an economical, environmentally safe, deposition process. By enlarging the potential market for the low voltage surrogate magnetron, more interest can be generated in the process development .

Solar cell process development is difficult to "debug" because solar cells are a multi element device. When a cell proves defective it is difficult to isolate the cause. Development of a surrogate magnetron YBCO process would be easier to "debug" than the same process development for solar cells. This is because YBCO is used for single element resistive devices with fewer aspects to analyze. And the resulting process could be directly transferred to solar cell production.

Methods and Materials

Magnet Design

Two computer simulation programs were used to design the magnets. Integrated Engineering Software Inc. of Winnipeg Canada makes a 2 D program called Magneto and a 3 D package called Amperes.

The 2D program was used to select the most efficient materials and orientations. The 3D package was used to design the end magnets at the turns in the race trace shaped magnetic assembly. It took two months to learn the software and to design the magnets.
The design process consisted of first entering a mechanical configuration and material parameters. Then the program simulated the resulting field. Three rules guided the design process:

Maximize the field.
Minimize the number of magnets
Minimize the size

A modular design was chosen to allow the field to be varied by removing some of the magnets and rearranging the pole pieces.

The next figure shows the final magnet assembly . The assembly is 160 mm (6.3") long, 25 mm (1") high and 50 mm (2 ") wide. The inner magnets are grade 30 which provides a relatively weaker central field compared to the outer magnets which are the stronger grade 40. This decreases the particle flux to the substrate giving an "balanced magnetron" effect. This was done because of concerns that the extremely concentrated target magnetic flux lines would be near the substrate. The inner magnets were already on hand and using them saved time and resources. The charged particle flux bombardment is moderate and is not harmful at present. Future design can certainly decrease this bombardment.

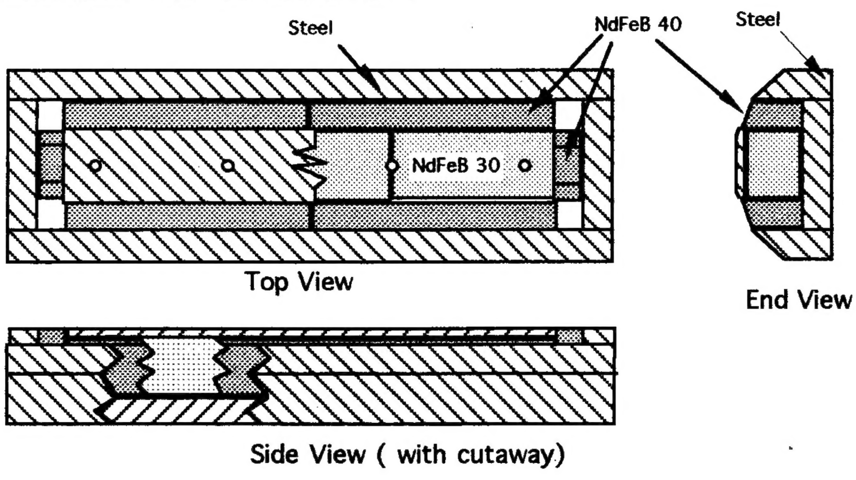

Figure 5 Final magnet array

A stronger 7500 Gauss design which used NdFeB grade 48 H was sent out for quotes. The response from the magnet companies suggested that grade 40H would be more suitable since it varied less with temperature and was mechanically stronger.

This lowered the 7500 field by less than 10%. The multiple magnet segments originally chosen could not be easily made in a timely manner. So a less efficient but more easily made assembly with fewer magnets was designed and made. 5500 gauss was the final level achieved.

The next figure shows the simulated magnet field in gauss. The peak field was about 5600 gauss. Some field lines were removed from the plot for clarity.

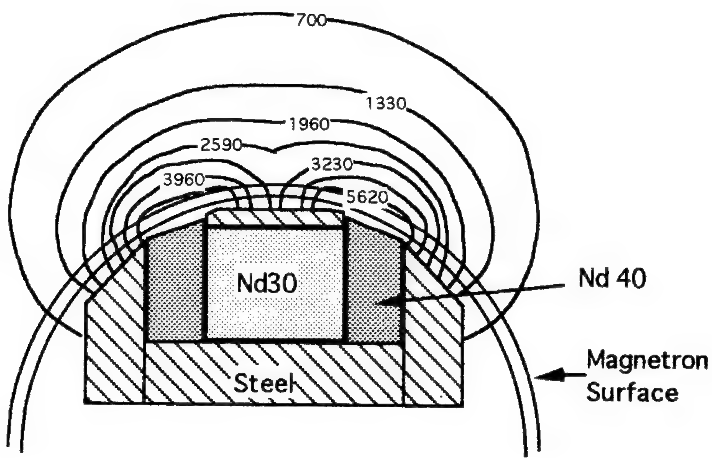

Figure 6 Radial plot of magnetic flux

Assembling the magnets was a challenge since they were so strong. Fingers can be injured if care is not taken. The best magnet configurations were those which repelled each other. These assemblies had to be held together with bolts to prevent them from repelling each other and dissembling the array.
The best configurations also had steel pole pieces on 3 sides. If there was no bottom pole piece, strong fields could still be achieved but a "ghost" field , that is, an extra ring of flux, was seen around the main field. Fields were visualized using "Magneview" film from Jobmaster Corp. This is a plastic sheet covered with metal particles in a plastic matrix. The normally dark green film turns light green at the inflection points, the strongest field points, of the magnetic assembly.

After assembly, the resulting field was plotted using a Gauss meter model GM-1A also from Jobmaster. A transverse probe type PT75, linear to 1%, was used to probe the fields. It has a sensing area of 1.5 x 3 mm set off from the tip by 2.2 mm.

The fields were plotted on the finished magnet assembled into the cylindrical magnetron. The Magneview film was placed under a transparent plastic film with a 1 cm x 1 cm grid printed on it. This "sandwich" of 2 sheets was taped around the cylindrical surface using the magnetic image in the magneview film to center the grid with the field.

The PT 75 probe was held in a non-magnetic wooden fixture which had 4 plastic feet arranged along an arc. This allowed the probe to be precisely positioned any where on the grid overlaying the cylinder.

Next, figure 7 shows how the magnetic field probe was held in position to make the magnetic field plots.

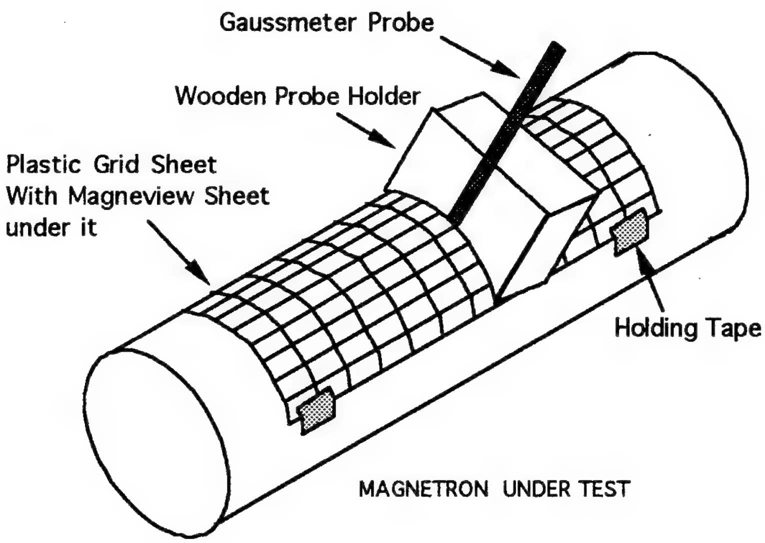

Figure 7 Method for magnetic field plots

The gauss meter sensing "spot" is 3 mm above the surface counting the 2.2 mm offset plus the thickness of the plastic sheets and clearance. Refer to the plot of Figure 4. Move from point A, 2900 gauss, to point B , 3 mm to the left. This gives a reading of 5500 gauss at the magnetron surface.
If the running clearance of 1 mm could be reduced to .3 mm and the cylinder wall thinned by .5 mm, we could move 1.2 mm further to the left to point C . Then 7000 gauss could be attained at the surface. This could be done in the next phase. This shows the extreme importance of a thin magnetron wall.

It also shows how much the magnetic flux level would change if a magnetron were coated with, say, a usual 9 mm of material on a 1.5 mm wall. When most of the material had been sputtered away, B would have increased from less than 1000 gauss to nearly 3000 gauss. It might be difficult to adjust the process parameters to compensate for such a change.

Figure 8 following is a plot of the best magnet assembly achieved. The plot values are uncompensated for the separation of the probe from the actual surface of the cylinder.. The readings must be corrected using the graph in figure 4.

1 x 1 cm grid

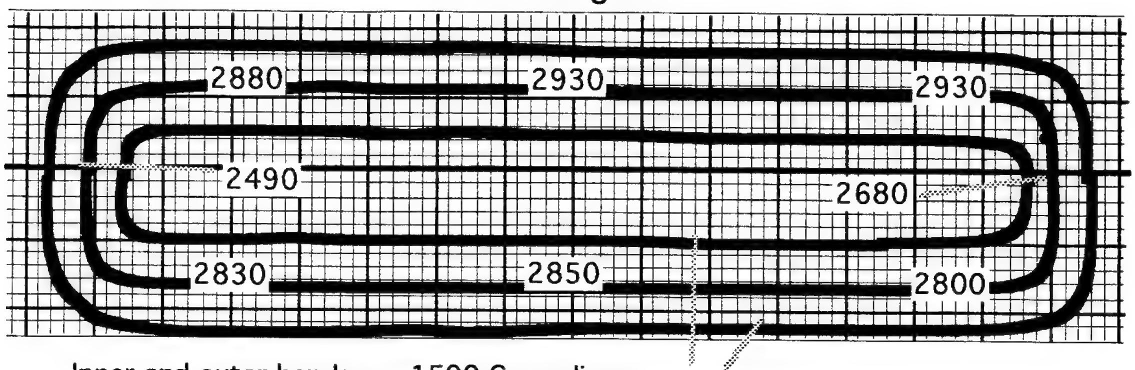

Inner and outer bands are 1500 Gauss lines

Figure 8 Magnetic field plot of final magnet array (uncorrected)

Magnetron Design and Assembly

A previous magnetron design was redesigned to accept the new magnets. As it turned out, this older magnetron was used for most of the experimental work. The new magnetron was delivered late because of defective materials supplied to the machinist. The new magnetron was to be used for chromium deposition. The older magnetron was used for three other materials, aluminum, tin, and stainless steel.

Since no auxiliary sources could be built on this contract, the tin and aluminum magnetrons had a thin coating to simulate the surrogate. The Al target was a 1.4 mm thick sleeve. The plasma sprayed tin target was 2.6 mm thick including the 1.4 mm thick Aluminum sleeve and the 1.2 mm Tin coating. The electroplated tin target was 2.1 mm thick with a 0.7 mm thick coating. The target core itself was used without a sleeve to deposit stainless steel. Because of these variations in magnet to target surface separation, the estimated maximum flux for each material was:

Stainless steel .... 5500 gauss
Aluminum......................... 4100 "
Tin.Electroplated .... 3600 "
Tin Plasma Sprayed ..... 3200 "

With the new magnetron design , all materials would have the same low magnet to material gap. Magnetic field strength would then be 5500 gauss for all materials.

The old magnetron was a 3 piece design with 4 "O" ring seals. It has a core tube, an end cap, and an outer sleeve . Two of the "O" rings seal between the outer sleeve and the core tube. Several sleeves were coated with various materials and used to change sputter material without changing the core tube.

A thin film of oil was used to transfer heat from the sleeve to the water cooled core tube. The problem with this older design was oil contamination of the outer sleeve surface. The outer sleeve had to be very carefully cleaned after sliding it over the core tube.

The new magnetron design was a two piece design without an outer sleeve. Its cost was lower so that the cost of several new magnetrons was about the same as one core tube plus several sleeves. 2 "O" ring seals were also eliminated making the new magnetron a significant improvement. Even though it was little used in this contract, it is a good design for the next phase

The two types of magnetron tube are shown in the next figure.

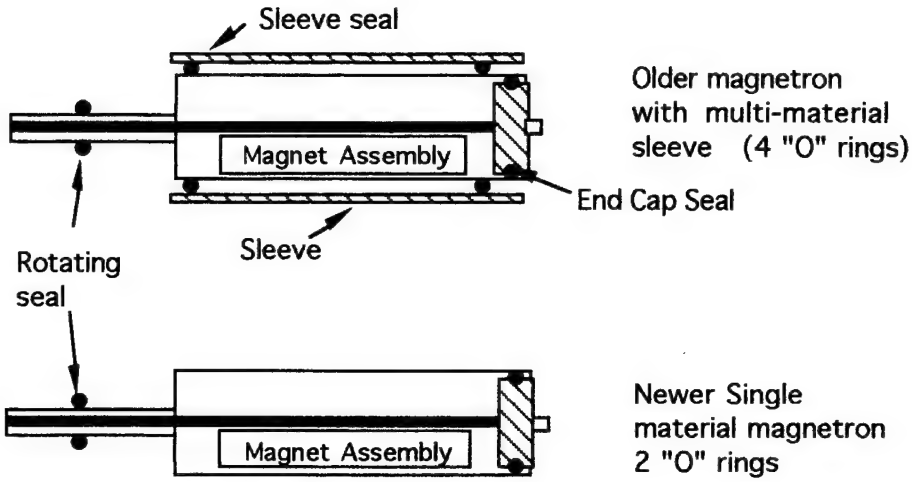

Figure 9 Magnetron designs

The magnetron tube is fitted into the deposition chamber as shown in this figure

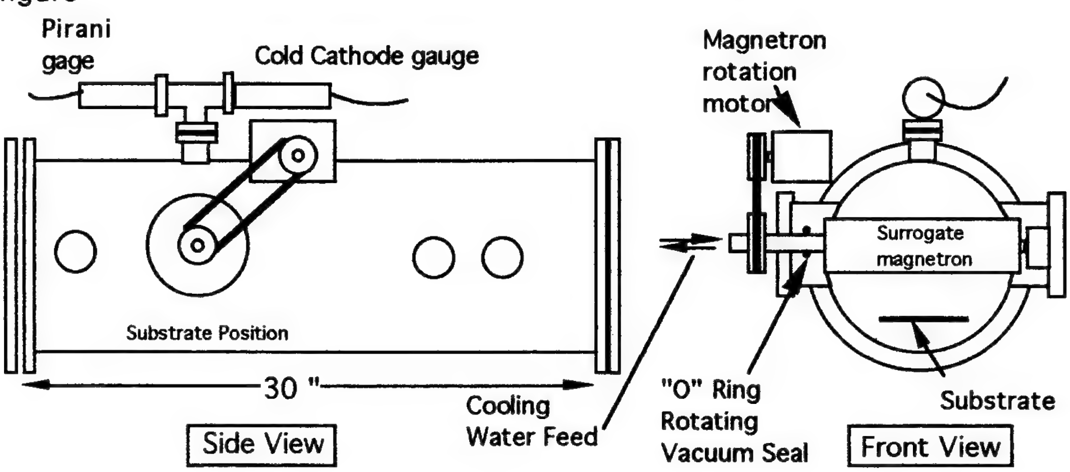

Figure 10 Deposition system with magnetron

Energy Probe Design

An energy probe was designed and built to measure the energy of incoming atoms at the substrate. It followed the design of Thornton [13]. The probe disc temperature increases at a rate proportional to the average energy of all incoming particles. If electrons or ions also hit the probe disc then the average energy will increase. A design improvement was made by using the two thermocouple wires sharpened to a point to contact the 25 mm diameter aluminum probe disc for measuring temperature rise. Since the thermocouple was not permanently attached, the probe disc could be removed for a film thickness measurement by the weight gain method.

Thus energy and deposition rate are measured in precisely the same spot. This noticeably improves repeatability over Thornton's method.

As long as there is no temperature difference between the two point contact, the law of intermediate materials assures an accurate temperature reading. The sampling probe was a 25 mm diameter aluminum disc 0.25 mm thick. It weighed about 300 mg. Weight gain was measured to 0.05 mg accuracy using a Christian Becker "Chainomatic" analytic balance. Typical weight gains were 1.8 to 2.2 mg. The overall repeatability was 5%.

The following figure shows side and isometric views of the energy probe.

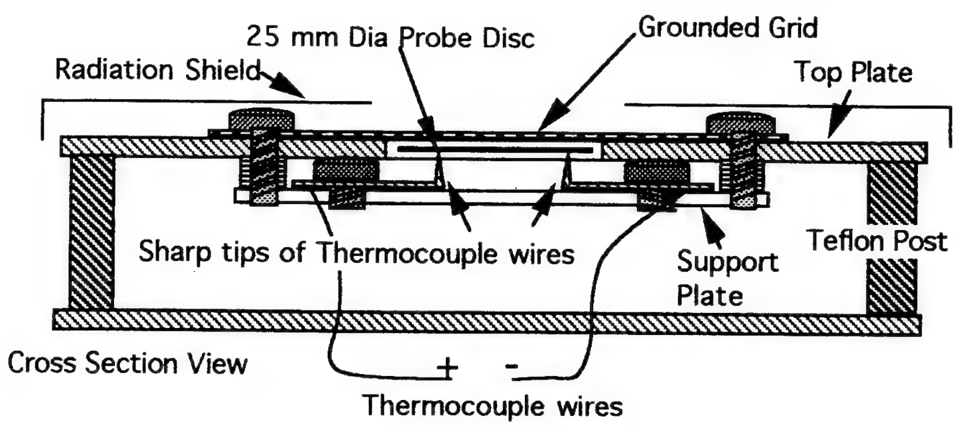

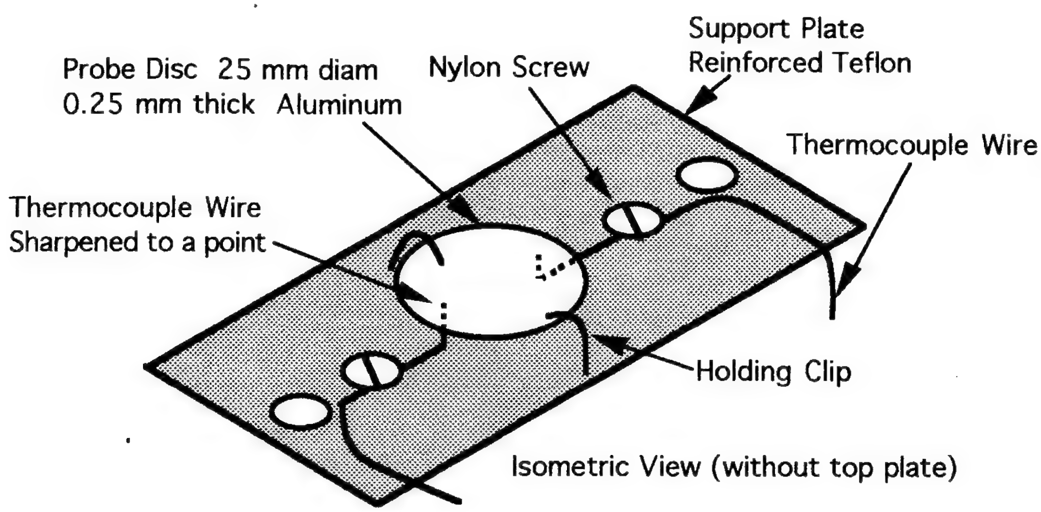

Figure 11 Energy probe

The energy probe was fitted with a grid and a radiation shield which could be biased to prevent either electron or ion bombardment.

A probe suitable for measuring negative ion bombardment was also designed and made. It follows the design of Brodie, Lamont, and Jepson [14] as modified by Rossnagel [15] It was similar to the energy probe except for 2 additional grids and a magnet. It is shown in the next figure

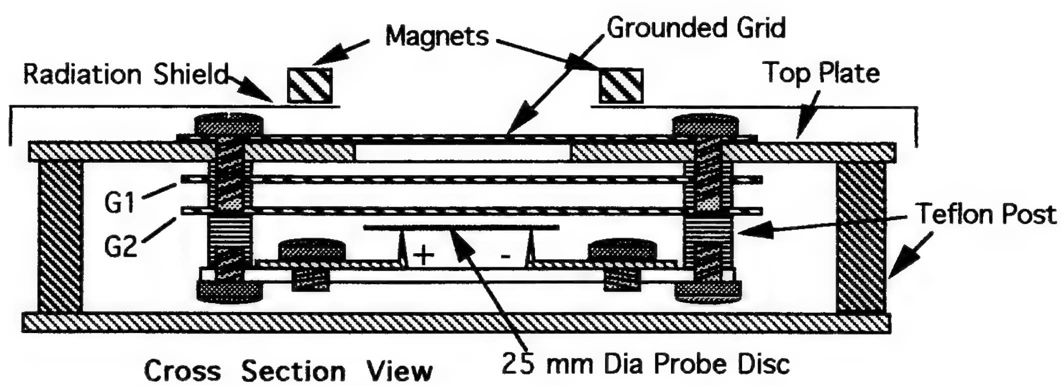

Figure 12 Ion Probe for high energy neutral detection

The main use of this ion probe is to detect secondary electrons emitted by any high energy reflected neutral particles. In this way the existence and quantity of such neutral bombardment could be measured. The neutrals do not directly contribute any current so they must be measured indirectly. The magnets eliminate electron bombardment by trapping them. Positive ions are eliminated by biasing grid G1 positive. The probe collector disc is biased more negatively than the target to repel any energetic secondary electrons from the target. Grid G2 is biased sequentially to plus and minus 80 V.

The current difference between the two bias polarities is attributed to secondary electrons emitted by high energy reflected neutrals.
This ion probe was built but not used since plasma voltage levels never reached the 100 volt level. The time was spent instead studying the low plasma impedance effect.

This was the method of use for the energy probe:

1. Weigh the probe disc to within 0.05 mg
2. Insert the disc into the probe housing and place the probe housing into the vacuum chamber under the magnetron.
3. Perform an electrical continuity check.
3. Pump down the system and then set the argon pressure.
4. Use a DVM accurate to 0.01 mv to measure thermocouple voltage.
5. Turn on the preset magnetron and measure the thermocouple voltage vs. time in 10 second intervals.
6. Sputter for 6 minutes at a selected current.
7. After sputtering measure the cool down curve.
8. Open the vacuum system, remove the probe disc and weigh it.

The formulas for converting the temperature rise rate and weight gain are derived in Thornton [13]. They are listed next along with a typical graph Fig.13, of temperature rise and fall.

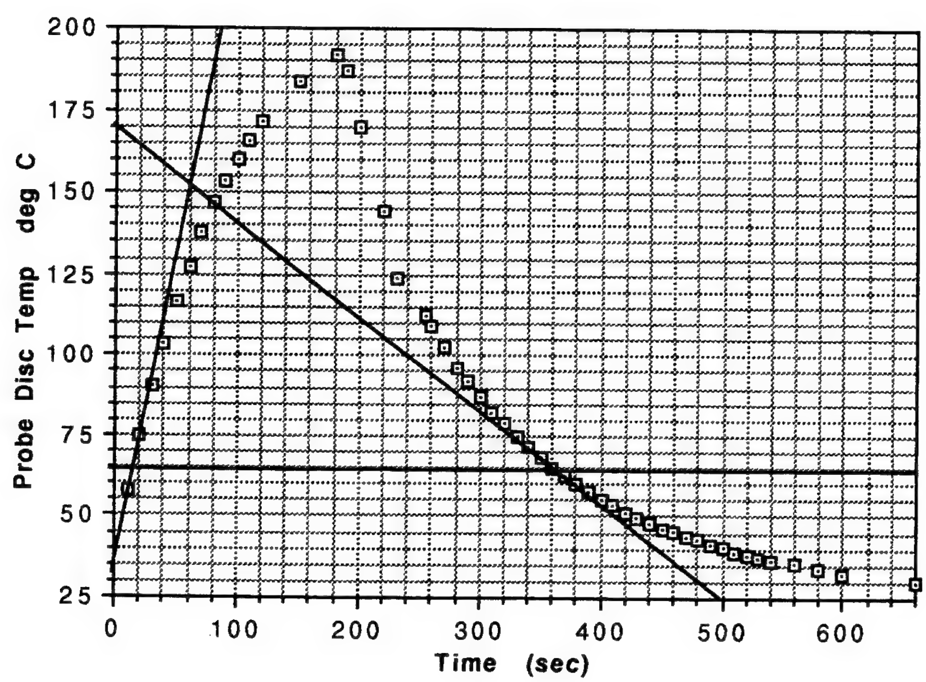

Figure 13 Typical energy probe dtemp/dtime curve

Calculation of ev/atom

Inputs

read from graph rate of rise (deg C/second) $=R_{on}$

rate of fall (deg C/second) $= R_{off}$

$R_{total} = R_{on} + R_{off}$ to be read at the minimum temperature allowing an accurate slope determination.

The total rate of increase is the sum of rise and fall since the rate of fall is how much the rate of rise is being decreased because of cooling effects.

The total weight W_t of the aluminum probe disc

The weight gain $= \Delta w$ deposition time $= t_d$

Calculation Process

Q = ev/second = W_t(0.215=specific heat...Al)(R_{total})/3.8 x 10^{-20} ev/calorie)

F = atoms/second = (Δw)(N_{Av}= 6 x 10^{23})/ (t_d)(56 = specific heat ..steel)

ev/atom = Q/F

Deposition System

The complete deposition system is shown next.

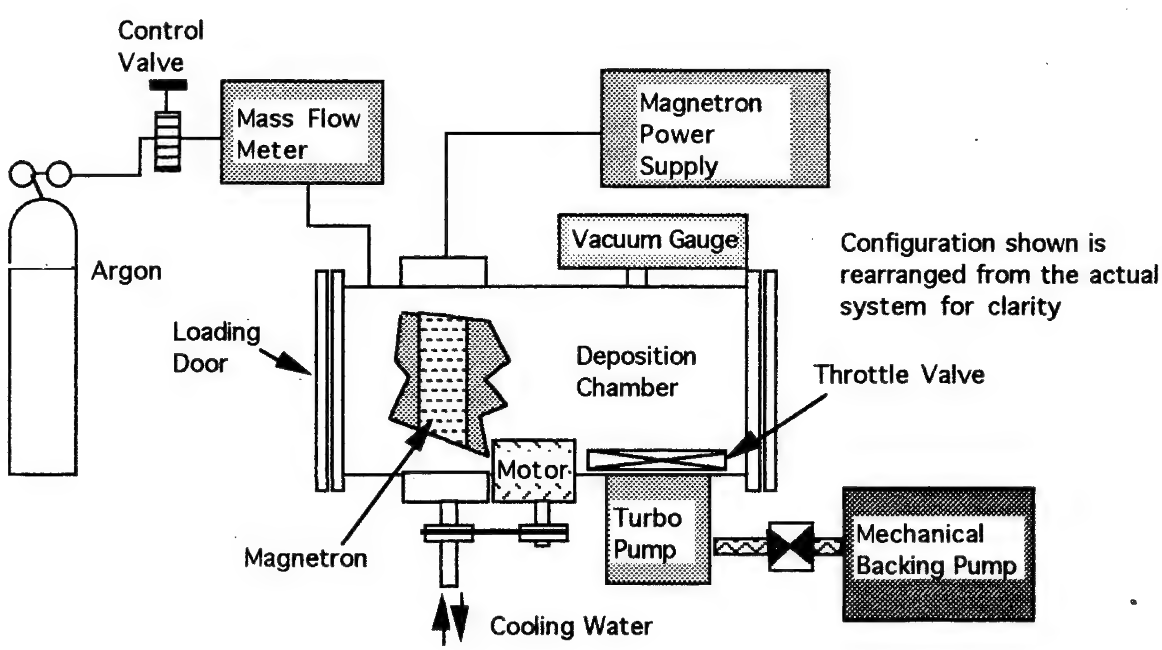

Figure 14 System diagram

System Specifications

Size.......................... 10" diameter 30 " length
Base Pressure............ 1 x10^{-5} torr
Gas Pressure Range ... 1 to 10 microns
Gas flow range............1 to 50 SCCM
3 gas feed line systems
Turbo Pump Speeds..... 66 and 170 Liters / second
Power supplies
Sloan SP 2/5   2.5 kW   4 amp .....single phase
Eratron 8210   dual range ....   3 phase
10 and 1   kW   2.5 and 25 amp

No three phase power is available to my lab. Instead, a 3 phase motor running with 220 V single phase fed to one phase winding generates quasi 3 phase power. The motor acts as a rotating transformer. Instead of three phases A,B, &C 120 degrees apart, the result is a 90 degree separation from A to B and a 180 degree separation from B to C. This provides fairly ripple free DC sputtering voltage from the Eratron supply. However, if the anodes are incorrectly placed the ripple goes to 100%. This phenomenon has been a useful guide in anode studies.

Base vacuum is measured with a cold cathode gage. Operating pressures from 1 to 10 torr are measured with a VRC pirani gage.
Pressure is controlled with gas flow and a magnetically coupled sliding shutter "throttle valve" which covers the turbo pump port and limits pumping speed.

The chamber is loaded and unloaded by unbolting the 10" diameter front blank off plate. A viewport located near the turbo and away from the sputter zone is used along with an 6 inch wide mirror to view the entire sputter zone.

IV curve method

The IV curves were generated with this procedure:

Pump down to ,2x10^{-5} torr. Sputter at 1 amp for 5 minutes to clean up the target.
The voltages are read starting at the lowest current and proceed to the highest currents. Data points are read and recorded manually. The entire curve, after the initial cleanup sputtering, takes about 3 minutes to generate.
The target rotated at 60 RPM. Target cooling water temperatures never exceed 25 degrees C.
An oscilloscope is used to monitor the power supply voltage to insure that voltage ripple is less than 10 %.

Results

Power supply and anode effects

There were two difficulties with the initial experiments. One was excessive ripple caused by the poor 3 phase mains power to an Eratron 3 phase sputter power supply. The net result of the ripple was uncertaintanty of the true effective plasma voltage. The other difficulty was insufficient clearance from the magnetron magnet to the chamber wall.

Fixing the insufficient clearance problem was relatively easy. The vacuum deposition chamber is small, 10 inches in diameter. By increasing the magnet to wall clearance from 1 inch to 2 inches on each side, the sputter process became much more repeatable and arcing was diminished. The main problem was becoming aware of the inadequate clearance

The ripple problem was more difficult. During the first experiments I found that by biasing the anode with 2% of the target voltage, I could greatly lower the plasma discharge voltage. Plasma voltages approached 100 volts. These measurements were done with the Eratron power supply.
Biasing the anode, as shown below in Figure 16 , would "lower" the discharge voltage. I reported some of these low voltages on the third status report.

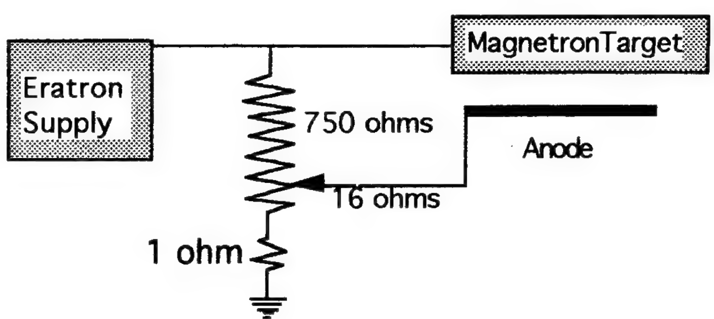

Figure 15 Anode for 'low" plasma voltage

As I found later, the anode bias was affecting the plasma in a manner I cannot yet explain. This caused the plasma voltage measurement to be uncertain. The Eratron requires three phase power but it was supplied with poor quality three phase mains power. Instead of the 120 degree phase to phase angle for input mains voltage, the power supply saw 90 and 180 degree phase angles. This phase error caused the ripple. Peak to peak ripple voltages were from ground to the full B- voltage. The ripple , per se, is easy to understand and was eliminated using an oscilloscope to monitor target voltage. But the following wave forms are not easy to understand.

First is shown the wave forms at the target and at the anode .

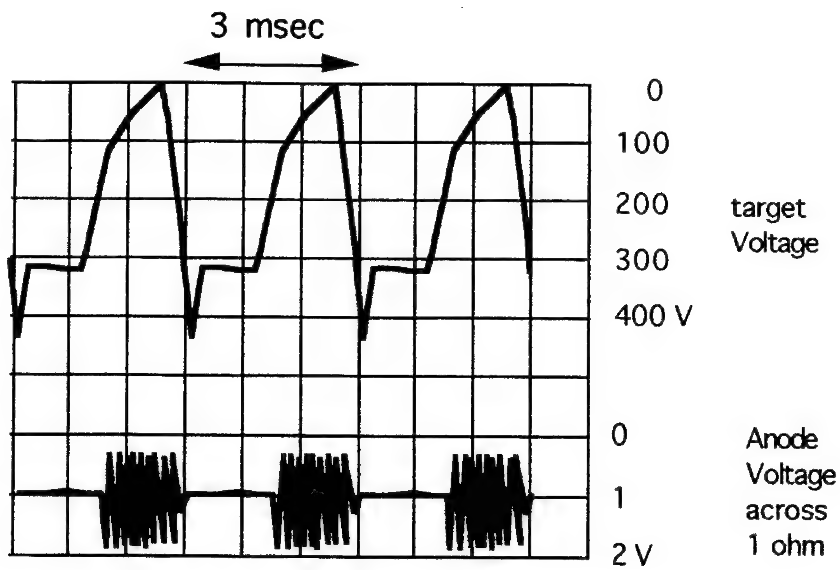

Figure 16 Ripple with power to anode

Next are the wave forms with the same anode connected to ground through the same 16 ohms but with B- disconnected from the resistive divider.

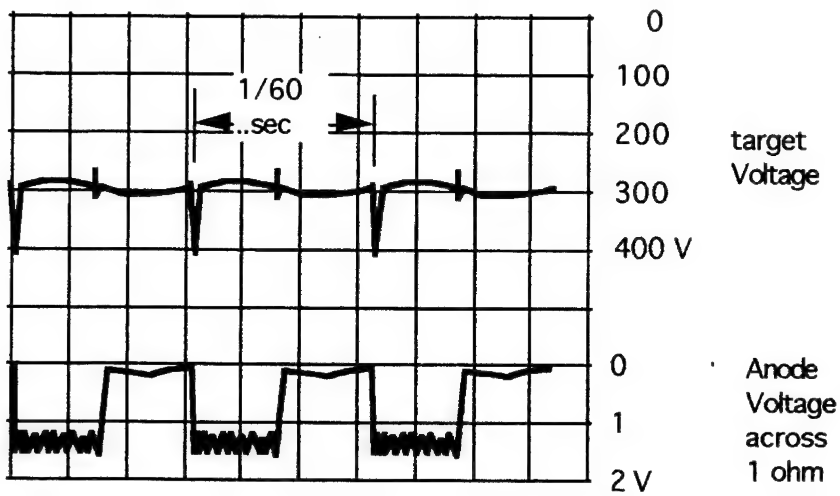

Figure 17 Ripple with no power to anode

There was a modulation of the plasma current as read through the voltage drop at the anode 16 ohm resistance to ground. At times, the anode current decreased when the target voltage increased.

Other times the anode current oscillated when the target voltage decreased. There may be some advantage to revisiting this anode effect when time and resources permit.

There were other anode effects as well. Placing the anode further from the plasma decreased the ripple. Stray magnetic fields on the side of the target ,90 degrees from the plasma, caused excessive ripple. Such "ghost" fields existed if there was no steel pole piece between the magnet assembly and the opposite side of the target.

With the anode was properly positioned and grounded, and with no "ghost magnetic fields, the plasma voltage ripple of the Eratron power supply decreased to less than 10%.

After discovering this ripple effect, I bought a Sloan single phase sputtering power supply and made another set of measurements with different anodes to verify these observations. This Sloan power supply had much less ripple than the Eratron. But improper anode placement and stray magnetic fields could still produce 20% ripple with attendant voltage errors.

Current vs Voltage (IV) Curve Data

The main result of this contract effort can be shown in the next graph:

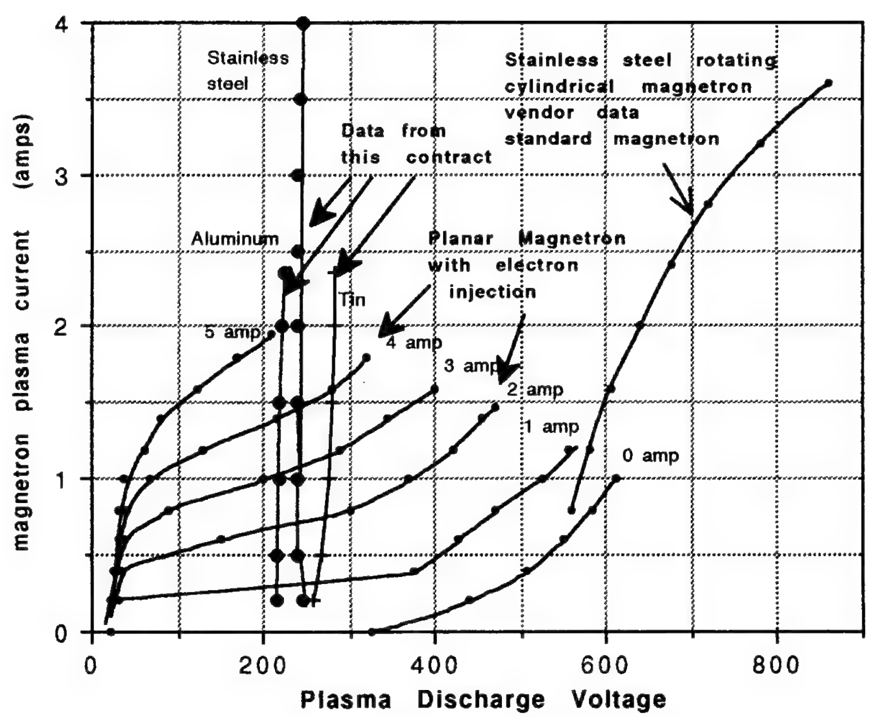

Figure 18 Major results of contract

There are 3 sets of data on the graph.

The first set is the six curves labeled 0 amps through 5 amps from data by Cuomo and Rossnagel [7]. The 0 to 5 amp labels refer to the injected electron current level for a standard planar magnetron .

Electron injection lowered the plasma voltage to 30 volts. This is encouraging data that proves low plasma voltages are possible. However, not much power could be applied to this magnetron. As the magnetron current increased above 20% of the injected electron current the plasma voltage increased. If low plasma voltage is desired high deposition rates must be sacrificed. The slopes of all the curves are large and are the same no matter how much electron current is injected. Such a large slope shows that electron containment is inefficient in this configuration.

The second set of data is a vendor supplied typical IV curve for a rotating magnetron available on the market. This magnetron IV curve was normalized to approximately the same total current as the other two magnetrons. These curves have approximately the same current per cm^2 values. The voltage is high, 600 to 800 volts, and slope impedance is also large.

The third set of data is three IV curves from this contract for stainless steel, aluminum and tin. While they do not start at 30 Volts as do the Cuomo and Rossnagel voltages, these IV curves have remarkably low impedance. These IV curves are nearly vertical. Voltage is nearly constant up to the current limit of the power supplies.

It's difficult to see on figure 18, but the stainless steel curve actually has a negative slope up to the 2 ampere magnetron current level. The tin at 3200 G and the aluminum targets at 4100 g were operating at significantly lower magnetic field strength than the stainless steel target. The tin and aluminum curves would shift to lower voltages if they were corrected for a constant magnetic field strength of 5500 gauss.

The next figure, 19 is a more detailed plot of IV curves for stainless steel and different magnetic fields and pressures. Both high magnetic fields and higher pressures lower the plasma discharge voltage significantly.

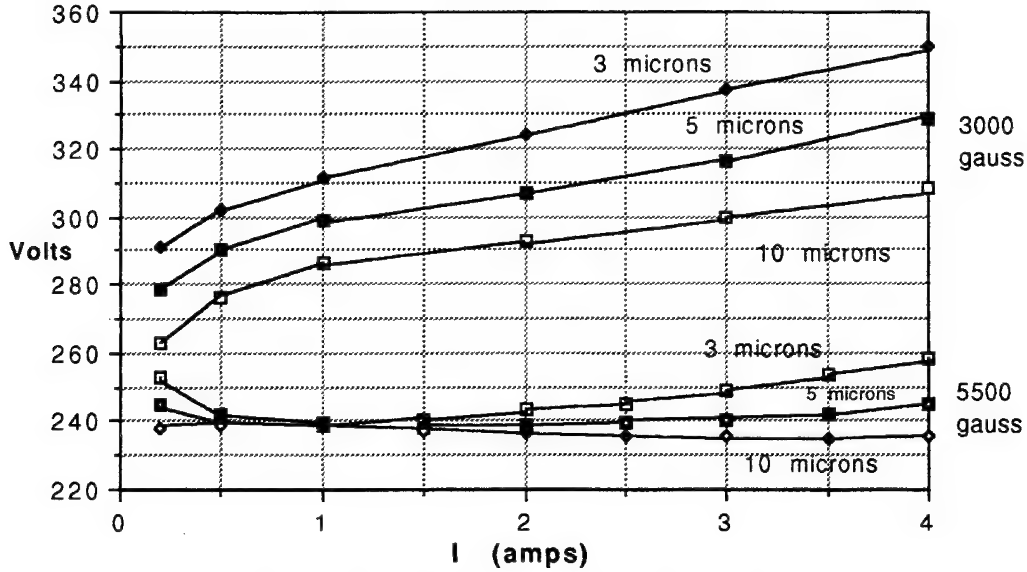

Fig 19 Stainless Steel IV curve

Note the negative resistance portion of the curve with the higher magnetic field

Next, figure 20 shows a different response for tin to the magnetic field. The slope or impedance for tin is higher than for aluminum and stainless steel.

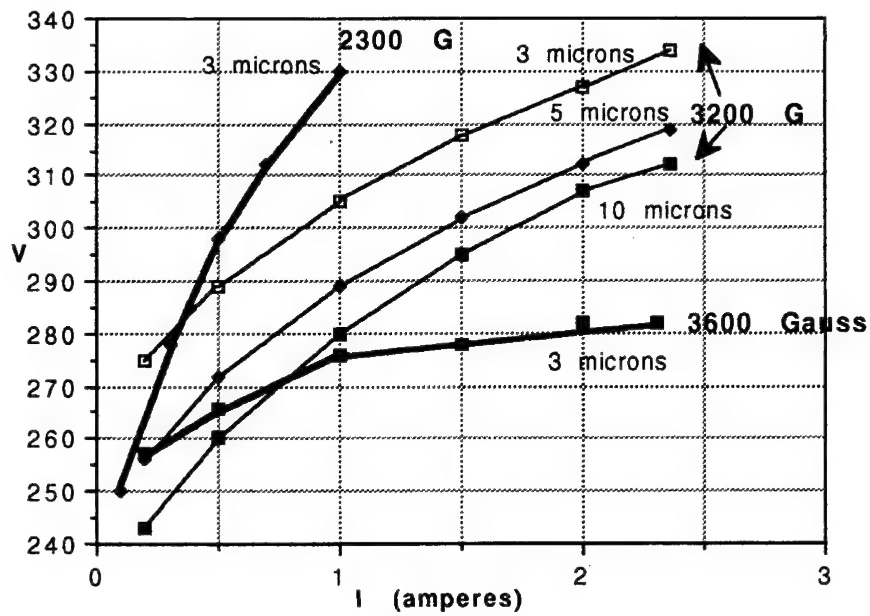

Fig 20 Tin I-V curve

For tin, the plasma voltage change with magnetic field seems non-linear. The 3200 Gauss curve was plasma sprayed tin and the 3600 g curve was electroplated tin. The type of tin may affect the plasma voltage but answering that question must wait until a later effort.

The aluminum IV curves, shown next, have an initial low voltage curve which then rises to a standard curve after several minutes of sputtering.

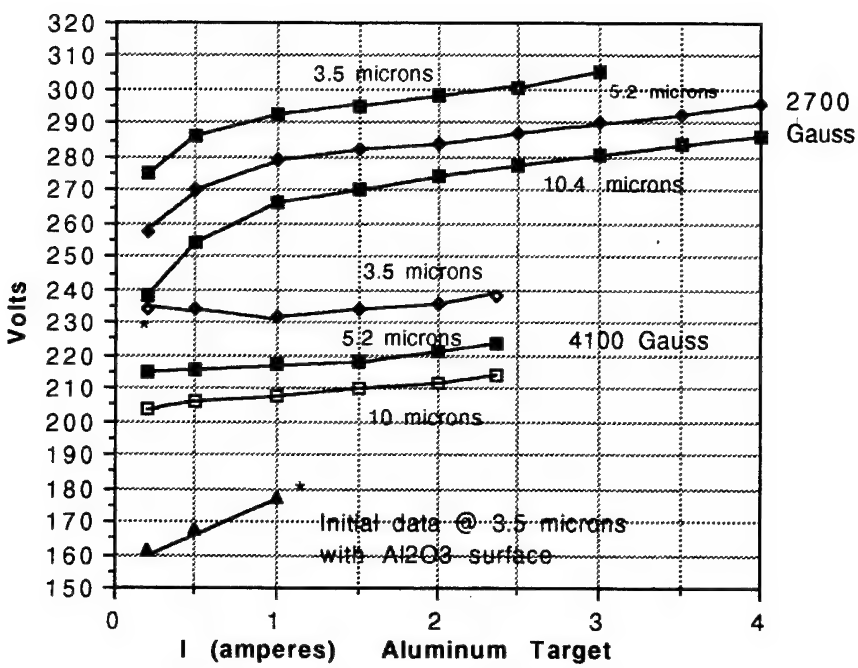

Figure 21 Aluminum I-V curve

The asterisk shows the initial curve and the final curve, both at 3.5 microns pressure and 4100 gauss magnetic field.

Since the secondary electron yield for a dielectric is higher than that of a pure metal , I infer that the low initial voltages is caused by more efficient secondary electron generation of the native oxide layer.

The 20 ohm slope of the initial curve may be partially the result of the native oxide layer thinning just before the oxide is completely sputtered away. All the other curves have slopes of about 5 ohms. The higher voltage, lower field, curves are logarithmic. The curves at the higher field are more linear with lower voltages.

It is worthwhile to see how these results compare to others who have studied the variation of plasma voltage with magnetic fields.

Figure 22 is a compilation of Gu and Lieberman [16] and Wendt et.al. [9] compared to some data from this contract There are some small discrepancies which I think are caused by different methods of calculating and measuring B. But the overall agreement is good

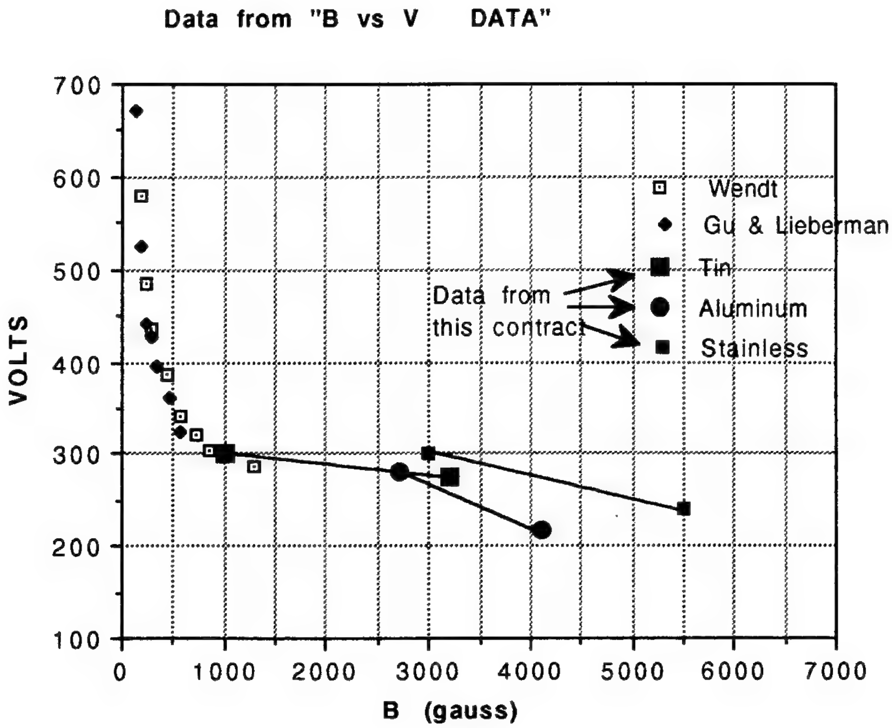

Figure 22 Data comparison with the literature

Energy Probe Results

I measured from 24 to 33 ev/atom. This energy was independent of magnetic field and plasma voltage in the 200 to 400 volts range. The lowest values were obtained with the radiation shield floating or negatively biased. The next curve , figure 23, shows the relationship of the initial temperature rise of the probe and the bias on the radiation shield which surrounded the probe disc. It indicates that most of the excess energy was caused by electron bombardment since the negative biases were most effective in reducing energy flux. These are moderate bombardment levels since the peak temperatures reached by the probe disc's small mass were usually no more than 120 degrees C during a 6 minute deposition.

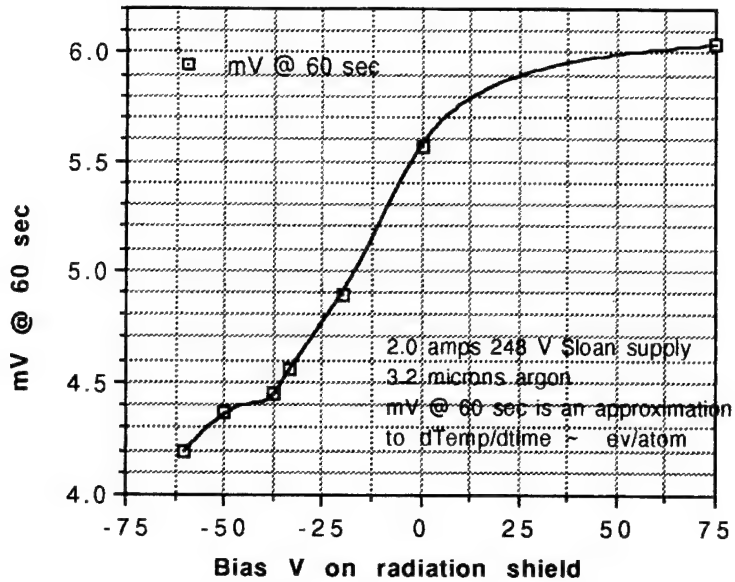

Figure 23 Bias effects on electron and ion bombardment

No ion probe data was taken since plasma voltage never got below 100 volts.

No chromium was deposited because the magnetron was delivered too late and there was no 100 volts plasma to use.

Discussion & Conclusions

The most important findings were the facts that voltage greatly decreased with higher magnetic fields and, just as important, that plasma impedance became very low. It seems reasonable to assume that combining electron injection into the magnetron plasma with a high magnetic field plasma will produce magnetron plasma discharge voltages below 50 volts and capable of high deposition rates. Present magnetrons sources on the market which use electron injection can provide low plasma voltages only at low powers. If such magnetrons are operated at more than 20 % rated power, the plasma voltage increases to levels seen with no electron injection...1,0000V for Copper and 500 V for Aluminum for example.

Some of the differences between the Al, Sn and SS I-V curves are due to different magnetic field strengths. Secondary electron yield is a weak function of most material and this also account for some of the differences.

There are two differences between Thornton's data and my data for the energy of iron atoms. Thornton determined 20 ev per atom while I got from 24 to 33ev for atainless steel. First there is moderate electron bombardment which added as much as 13 ev. Second, the 4 ev difference remaining. could be caused by uncertainty in determining where to read the rate of rise from the temperature vs, time graph. Using a recorder instead of manual data logging would help here.

The energy probe data showed moderate electron bombardment. When the grid and radiation shield in front of the probe were biased positively they drew a current of several amps. When the grid and shield were biased negatively they drew a fraction of an amp. This shows that while there is both electron and ion bombardment of the probe the electron current is larger.

This electron and ion bombardment is due to the stronger magnetic fields which extend from the target to the probe. The bombardment is not severe. The grounded grid in front of the probe dropped the ev /atom from 33 to 24 ev/atom . Thornton saw 20 ev/atom in his tests at even higher plasma voltages. Thornton's magnetic fields were around 200 to 400 gauss. By balancing the inner and outer magnetic field densities I should be able to noticeably reduce and even eliminate electron bombardment.
The rate of temperature increase seemed to be constant for the first 10 or 30 degrees of rise. On the other hand, the temperature decrease curve was very sensitive to the temperature level. This tended to increase the ev/atom numbers perhaps 5 to 10% high. The temperature-time curve shapes are more exponential than Thornton's, which were more nearly straight lines.

The goal of this contract was to reach plasma voltages less than 100 V. Magnetic fields of 3200 to 5500 gauss did not achieve 100 volts plasmas by themselves. I feel that 10,000 gauss can be achieved as magnet design experience is gained. However, looking at Figure 22, it is difficult to visualize any linear extrapolation to 10,000 gauss producing plasma voltages much below 200 volts. The extrapolation may be non linear, so the experiments should be performed

But by enabling efficient electron injection, high magnetic fields make it very possible to reach low voltages. These low voltages should produce self bombardment . Low voltages will certainly eliminate the negative ion bombardment problem. Of equal importance, low voltages can greatly decrease the temperatures needed for deposition and annealing.

It is important to again stress the difference between negative ion bombardment, positive ion bombardment, and self bombardment. Self bombardment describes the situation where the incoming atom has sufficient energy , 1 to 10 ev, to form a thin film layer of epitaxial quality at the instant of deposition [11].

As opposed to negative ion bombardment, positive Ion bombardment is beneficial because positive ions have low energy , about 1 to 10 ev. With positive ion bombardment, the incoming atom has insufficient energy to form a high quality film but additional energy is imparted to it by a third body, an accompanying positive bombarding ion (usually argon). This ion bombardment can greatly improve some mechanical and optical films, but it is not usually adequate for semiconductor films. Ion bombardment disrupts the damaging columnar growth structure and densifies the film which is beneficial. But it also can affect stoichiometry and is known to resputter material and induce high stresses. Positive ion bombardment does not seem likely to promote epitaxial quality films.

Applications to Phase II.

A phase II effort to deposit YBCO with on-axis sputtering would consist of the following tasks. A key aspect would be to start with a known standard YBCO process and then to change only one process parameter at a time.

1. Design and build a surrogate magnetron deposition system with 3 auxiliary planar magnetrons to deposit YBCO. The system would include a high temperature substrate heater for the initial experiments. The main technical challenge would be incorporating electron emitters into the high magnetic field environment of the surrogate magnetron. None of the auxiliary magnetrons would need electron injection or high fields.

2. Start the experiments by duplicating all aspects of a known successful YBCO process with one exception, the use of on-axis sputtering. All other critical process steps including the substrate type , the deposition and annealing temperatures, and the cool down cycles times and atmospheres would be unchanged. The magnetron process parameters such as elemental ratios and system pressures would be adjusted to maximize YBCO quality.

3 When acceptable YBCO was deposited, the next process parameter would be changed. Most likely it would be deposition temperature. And so on until all possible improvements had been achieved.

The major goals of a phase II effort would be :

1. On-axis sputtering proven.
2. Deposition temperatures lowered to allow the use of lower cost substrates.
3. Film improvement by precision stoichiometry control
4. Annealing temperatures noticeably lowered

Any process improvements developed for YBCO would be immediately applicable to several other materials such as thin film chalcogenide solar cells such as CdTe and Copper Indium Diselenide.

Commercial Applications

The surrogate magnetron could serve several very large markets:

High T superconductor thin films

This film solar cells such as CIS and CdTe

Flat Panel Displays

*Low temperature poly Si thin films (using a high temperature surrogate magnetron and CVD to deposit Si onto the surrogate. The Si would then be resputtered onto a low temperature substrate)

*Large areas arrays of vertical LEDs (Light emitting diodes)may be possible. When used with ferroelectric time sequential color filters, this would eliminate the need for printed color filters. Color filter lithography accounts for nearly half the cost of an FPD

Photo sensor arrays of HgCdTe

An expanded range of thin film semiconductors for new uses

A final important aspect of the surrogate magnetron is its environmental friendliness. It doesn't need toxic gases such as H2S etc. for the deposition of chalcogenide films. III-V materials such as GaAs,InP, InAs, and In Sb could also be synthesized directly from the elements. Toxic arsine, stibnine, and phosphine would not be needed.

Bibliography

1. J. Geerk et.al "HTSC Thin Film Growth by Inverted Cylindrical Magnetron Sputtering" Journal of Superconductivity, Vol 5 No. 4 1992 345-351

2. J.R. Gavaler " Critical Parameters in the Single-Target Sputtering of $YBa_2Cu_3O_7$ " J. Appl. Phys. 7 0 (8) Oct. 1991 4383-4391

3. Cuomo et al J. Vac. Sci. Technol. 15, 281 (1978)

4. Hammond "Thick Film YBCO for Wires and Tapes: Scale Up Issues and Cost Estimates" in "Advances in Superconductivity VIII " P 1029 Springer Verlag

5. "Tri-Mag" trade mark of L.M. Simard Inc. Bend, Oregon 97702

6. Howson "Reactive Ion Plating at Low Ion Energies with an Unbalanced Magnetron " *Vacuum* /vol. **4 4**/nos. 3&4/pp191-195 (1993)

7. Cuomo & Rossnagel "Hollow Cathode Enhanced magnetron Sputtering" J. Vac. Sci. Technol. A **4**(3) May/Jun 1986 pp 393-396

8. Thornton ..page 96 in "Thin Film Processes" Ed. by Vossen & Kern Academic Press 1978

9. Wendt & Lieberman "Spatial Structure of a Planar Magnetron Discharge" J. Vac. Sci. Technol. A **8** (2) Mar/Apr 1990 pp 902-907

10. Ishibashi "Low Resistivity ITO Transparent Conductive Films. II. Effect of Sputtering Voltage on Electrical Properties of Films" J. Vac. Sci. Technol. A **8** (3), May/Jun 1990 pp 1403-1406

11. K.-H. Muller " Role of Incident Kinetic Energy of Adatoms in This Film Growth" Surface Science 184:L375 (1987) Note...Chapter 21 of "Handbook of Plasma Processing Technology" Ed. by Rossnagel Cuomo and Westwood contains an excellent discussion of this subject of self sputtering, especially PP 506-509 as well as a good bibliography.

12. Window & Savides " Charged Particle Fluxes from Planar Magnetron Sputtering Sources" J. Vac. Sci. Technol. A **4**(2) , Mar/Apr 1986 p 196

13. Thornton "Substrate Heating Rates for Planar and Cylindrical-Post Magnetron Sputtrering Sources" Thin Solid Films, **119** (1984) 87-95

14. Brodie et.al "Production of High Energy Neutral Atoms by Scattering of Ions at Solid SurfAces and its Relation to Sputtering" Phys. Rev. Lett. Vol 21 #17 pp 1224-1226

15. Rossnagel "Energetic Particle Bombardment of Films During Magnetron Sputtering" J. Vac. Sci. Technol. A **7** (3) May/Jun 1989 p 1025-1029

16. Gu & Lieberman "Axial Distribution of Optical Emission in a Planar Magnetron Discharge" J. Vac. Sci. Technol. **A** 6(5) Sep/Oct 1988 pp2960-2964